communications biology

A Nature Portfolio journal

Article

https://doi.org/10.1038/s42003-025-09095-4

Microbial influx during early postnatal life fortifies the ocular surface and guards against allergic eye disease in mice

Yanbo Liu[1,7], Hang Sun[2,7], Shulin Song[1,7], Xiezhou He[1], Han Wu[1], Shangkun Ou[1], Hui He[1], Rongrong Zong[1], Yongxiong Chen[1], Guo Fu[3], Yiqiang Wang[4], Huping Wu[1], Andrew J. Quantock[5], Zuguo Liu[1,6] & Wei Li[1,6]

Host-microbiome interplay during development governs the homeostasis of various bodily surfaces, however, postnatal colonization of the microbiome and its impact on the homeostasis of ocular surface is still unclear. Here, the changes of the conjunctival microbiome in C57BL/6 J mice were tracked in 1-week-old neonates through to 8-week-old adult mice. This disclosed that changes in the conjunctival microbiome correlate with age, especially at the 2-week and 3-week time points, which, respectively, are accompanied by eyelid-opening and weaning. Antigen presenting cells were also recruited to the conjunctival epithelium after eyelid-opening, whilst an inhibition of microbial colonization at 2-to-3 weeks of age led to a disruption of mucosal homeostasis and aggravated the development of allergic eye disease. This study improves our understanding of the development of the conjunctival microbiome in mice, and provides an indication that early microbial colonization is required for the establishment of mucosal ocular surface homeostasis, the perturbation of which leads to increased susceptibility to allergic eye disease.

The ocular surface is continuously exposed to the outside environment, with the conjunctiva naturally harboring low numbers of live bacteria[1]. Although many studies have reported correlations between the composition of microbiota in the ocular surface and various physiological indicators and disease manifestations in adults[1–3], only a few have investigated the compositional characteristics of the ocular microbiome in children. Studies conducted on newborns have found that *Proteobacteria* was the dominant phylum in the ocular surface microbiome, followed by *Actinobacteria* and *Firmicutes* as the next two most abundant phyla[4]. In children under 18 years of age, *Firmicutes* and *Bacteroidetes* were the next two most abundant phyla after *Proteobacteria*. In comparison, the ocular surface microbiome in adults exhibited decreased abundances of *Firmicutes* and *Bacteroidetes*[5,6]. These studies suggest that the ocular surface microbiome varies across different age stages, however, the dynamic change of the microbiome of the ocular surface from early neonatal stages onwards has not been investigated. Here, we investigate the ocular surface microbiome of the mouse eye, which represents a good model system because the eyelids remain closed for 12–14 days after birth, allowing for continuous observation of the colonization of the ocular surface microbiome.

Antibiotic eye drops are commonly used in the treatment of bacterial infections of the ocular surface. However, because the clinical diagnosis of infectious, bacterial eye diseases in children is more difficult than in adults, the use of antibiotics might not always be the best course of action[7]. Even in the absence of ocular surface infection, given the susceptibility of newborns to pathogens, antibiotic eye drops have been widely used to provide ocular prophylaxis at birth for more than a century[8,9]. It is well known that topical antibiotics applied to the eye can affect the ocular surface microbiome, so early antibiotic use may have an impact on ocular surface microbial colonization and needs to be more thoroughly understood.

From birth onwards, the colonizing microbiome of human mucosal surfaces induces the development and maturation of immune cells and tissues that facilitate tolerance to environmental exposures. The composition of those microbial communities, meanwhile, changes considerably during the development of the immune system[10–12]. In both humans and

[1]Xiamen Eye Center and Eye Institute of Xiamen University, Fujian Provincial Key Laboratory of Ophthalmology and Visual Science, School of Medicine, Xiamen University, Xiamen, Fujian, China. [2]State Key Laboratory of Marine Environmental Science, College of Ocean and Earth Sciences, Xiamen University, Xiamen, Fujian, China. [3]Cancer Research Center of Xiamen University, School of Medicine, Xiamen University, Xiamen, Fujian, China. [4]Wisdom Lake Academy of Pharmacy, Xi'an Jiaotong-Liverpool University, Suzhou, Jiangsu, China. [5]School of Optometry and Vision Sciences, Cardiff University, Cardiff, Wales, UK. [6]Department of Ophthalmology, Xiang'an Hospital of Xiamen University, Xiamen, Fujian, China. [7]These authors contributed equally: Yanbo Liu, Hang Sun, Shulin Song. e-mail: wei1018@xmu.edu.cn

mice, a paucity of bacteria in early life leads to immunological defects that can be sustained into adulthood and increase the susceptibility to, or exaggeration of, allergic disease[13,14]. Such early-life events have been proposed in other mucosae[15,16]. Due to ethical concerns and the availability of limited numbers of samples in humans, the analysis of the microbiome of the ocular surface and its role in the development of ocular surface immunity in early life remains elusive. Accordingly, to test our hypothesis that alterations in microbial composition, or depletion of the microbiota early in life, may lead to perturbations of ocular surface immune homeostasis, we have investigated the ocular surface microbiome of mice at six different growth stages between postnatal weeks 1-to-8 weeks. We also explore the likelihood of dysbiosis of ocular surface microbiota during early postnatal life induced by the use of antibiotics and its impact on ocular surface homeostasis.

Results

Postnatal dynamic changes of the conjunctival microbiome

To understand the relationship between the ocular surface microbiome and the ocular mucosa, we first characterized the conjunctival microbiome in mice between 1 and 8 weeks of age using 16S rRNA sequencing for bacterial identification. A total of 6682079 16S rRNA tags were obtained with an average of 105993 effective tags across samples (Table S1) and then we clustered 646 OTUs based on 97% sequence identity. OTUs associated with negative controls were removed from the analysis based on the indicator value (IndVal) index, employed for the identification of potential contaminants as described previously[17]. Community bar-plot analysis displays relative levels of the conjunctival microbial community in all 60 samples at the phylum level (Fig. S1a). A core microbiome consisting predominantly of *Proteobacteria*, *Firmicutes*, *Actinobacteria*, *Chloroflexi*, *Acidobacteria*, *Patescibacteria*, *Cyanobacteria* and *Verrucomicrobia* phyla was found, accounting for up to 85% of sequences on average. At the family level, the composition of the top ten microbials in mouse conjunctival tissue changed during eyelid-opening. In particular, at 2- and 3-week of life, the conjunctival microbiome underwent transient alterations as *Enterococcaceae* and *Staphylococcaceae* outgrew *Moracellaceae* and *Bacillaceae* (Fig. 1a). Meanwhile, at the genus level, composition and SIMPER analysis indicated that *Staphylococcus* and *Enterococcus* were significantly enriched in 2- and 3-week-old mice, while *Acinetobacter* and *Anoxybacillus* changed in an inverse direction (Fig. S1b and Table S2). BugBase was used for phenotypic prediction analysis, which revealed that the relative abundance of predicted potential pathogenic bacteria was highest in 3-week-old mice (Fig. S1c). We further examined the changes of conjunctival microbial diversity across different developmental stages. The Shannon index depicted a slight decrease in α-diversity in 2-week-old mice, followed by a dramatic decrease at 3 weeks of age. Thereafter, α-diversity increased until the 4-week of age and remained relatively constant until 8 weeks (Fig.1b). A PCoA was performed to visually depict the variations in taxon composition among these mice. In 4- to 8-week-old mice, β-diversity returned to levels similar to the initial microbial diversity observed in 1-week-old mice (Fig. 1c). No significant difference in α-diversity was observed between males and females across all samples. During postnatal development, both sexes exhibited a transient decrease in α-diversity at 3 weeks of age, while the Shannon index remained relatively stable at 1, 2, 4, 6, and 8 weeks, with no significant differences observed (Fig. S1d). These results indicated that male and female

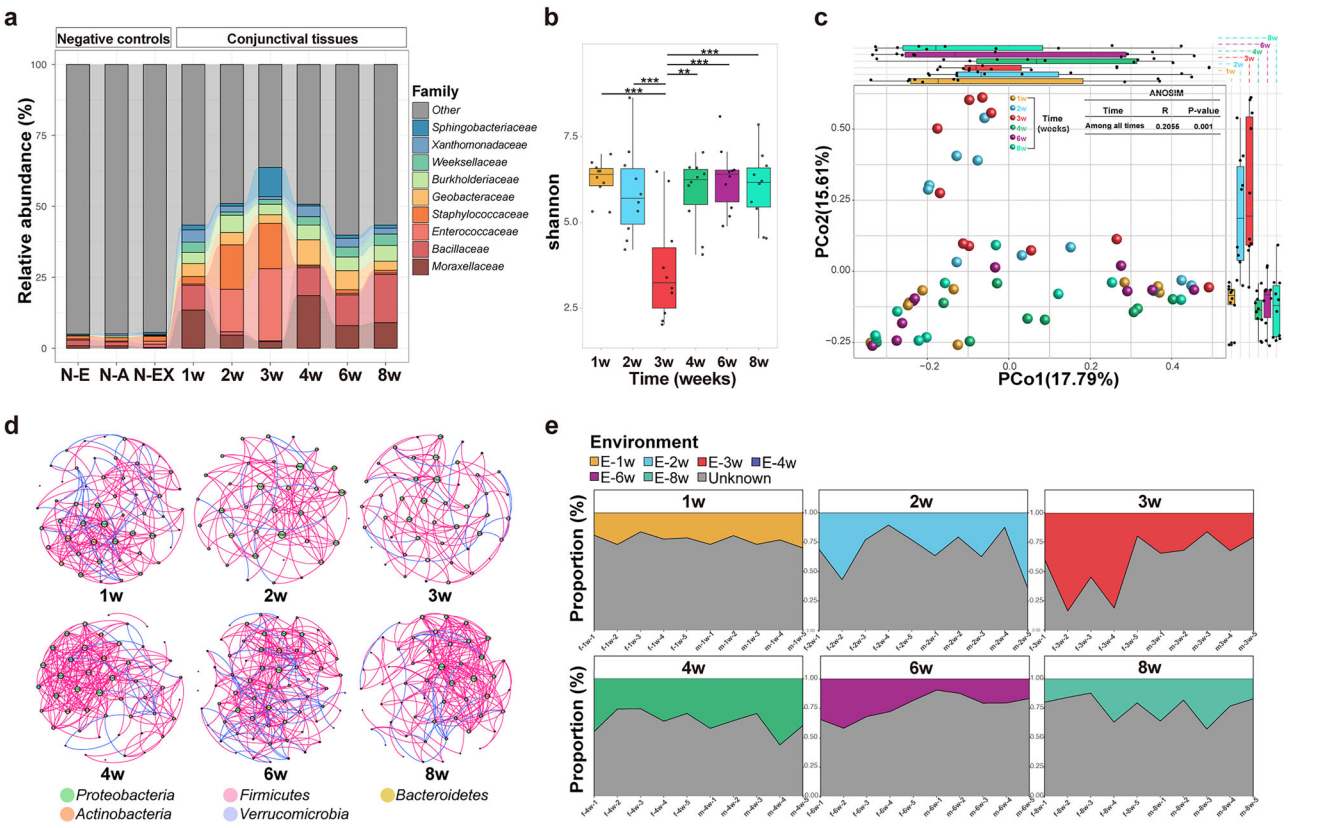

Fig. 1 | Dynamic changes in the conjunctival microbiome of mice aged between week 1 and 8 of neonatal development. a The average relative abundance at family level (top 10) of the conjunctiva across different developmental stages in mice ($n = 10$ per group). Negative controls include laboratory environmental samples (N-E), reagents used at the time of amplification (N-A) and blank extractions (N-EX). **b** Shannon index of the conjunctival microbiome across different developmental stages in mice. **c** Principal coordinate analysis plot generated using OTU metrics based on the Bray-Curtis dissimilarities. Each point represents a sample. **d** Networks of co-occurring bacterial OTUs in conjunctiva across the different developmental stages in mice, based on the correlation analysis. The co-occurring networks are colored by phylum. A red edge indicates a positive interaction between two individual nodes, while a blue edge indicates a negative interaction. **e** Tracking the source of conjunctival microbiome across different developmental stages in mice. Data are shown as mean ± SEM. $^{**}P < 0.01$, $^{***}P < 0.001$ using the one-way ANOVA.

mice display a similar pattern of microbial diversity changes during developmental stages. In contrast, significant variations occurred based on gender as identified by the β-diversity index (Fig. S1e).

We next explored bacterial co-occurrence patterns among mice at the six time points using network analysis as previously reported[18]. In these six networks, positive correlations were much higher than negative correlations (Fig. 1d and Table S3). Overall, the analysis of topological properties in these empirical networks revealed a significant difference between each age group (Table S3). Further comparison of co-occurrence patterns across six aggregate fractions showed that the bacterial community exhibited closer correlations (for example, a higher number of nodes) in the 1-, 4-, 6- and 8-week-old mice, while the 2- and 3-week-old mice showed a lower correlation (Table S3). Additionally, the data for average path length (APL) and average clustering coefficient (avgCC) indicated that the empirical network in 1-, 4-, 6-, and 8-week-old mice featured a more prominent "small world" module (Table S3). Subsequent structural analysis revealed the prevalence of deterministic co-occurrence patterns in the bacterial networks at intra-phyla level. Notably, bacterial OTUs in the predominant phyla, including *Proteobacteria*, *Firmicutes*, *Bacteroidota*, *Actinobacteriota*, and *Verrucomicrobia* exhibited a stronger propensity for co-occurrence compared to other phyla (Fig. 1d).

Due to the complex living environment of mice, the ocular surface microbiome may be affected by the animals' surroundings during eyelid-opening. In order to track the potential source of the conjunctival microbiome, we examined possible origins, including feces samples in cages (Table S1). This indicated a significant difference in β-diversity between the conjunctival microbiome and environmental microbiome (Fig. S1f). The results of the microbial source tracking (FEAST) revealed that the microbes of the conjunctiva in 2- and 3-week-old mice likely mainly originate from the living environment (Fig. 1e), thus, we suspect that the mouse conjunctival microbiome is instantaneously affected by environmental factors at the time of eyelid-opening.

Antigen presenting cells (APCs) are transiently recruited in the conjunctival epithelium in early postnatal life

Given that the conjunctival microbes undergo instantaneous change during eyelid-opening, we speculated that microbial colonization during this period will have a major impact on the recruitment of immune cells in the conjunctiva. Evaluation of whole-mount conjunctival tissues by confocal microscopy, indeed, demonstrated a dramatic increase of $CD45^+$ cells in the conjunctival epithelia of 3-week-old mice compared to the conjunctival epithelia of 1-, 2-, and 4-week-old mice (Fig. 2a, b). Further analyses by flow cytometry showed that the numbers of $CD45^+$ cells in the conjunctiva dynamically changed, where it increased from 1 to 3-weeks, peaked at 3-weeks, and declined thereafter by 4-weeks (Fig. 2c). We suspected that some of these cells emerging in conjunctival epithelium could be APCs because many cellular dendrites were visible (Fig. 2d). Since APCs can be characterized by the expression of CD11b, CD11c, and MHC II[19], we performed immunostaining on whole-mount conjunctival tissues and found a significant increase of intraepithelial $CD11b^+$, $CD11c^+$, and MHC II^+ cells in the conjunctiva of 3-week-old mice (Fig. 2e), suggesting an enhanced recruitment of immune cells in the mouse conjunctival epithelium during eyelid-opening.

Maturation of the conjunctival epithelium during postnatal eyelid-opening

In mice, initial conjunctival epithelial stratification occurs around the time of eyelid-opening when the conjunctiva is first exposed to light, oxidative and environmental stress[20]. The 1-to-2 cell layer-thick conjunctival epithelium in 1-week-old mice has become increasingly stratified and, respectively, has formed a squamous epithelium 3-to-4 cells thick and 5-to-6 cells thick in 2- and 3-week-old mice (Fig. 3a). The gradual increase of epithelial thickness was further confirmed by immunofluorescence staining using antibodies to conjunctival epithelial specific marker Krt19 and tight junction protein ZO-1 (Fig. 3b). The conjunctiva is a mucosal tissue, rich in mucin-producing goblet cells. In the mouse conjunctiva, goblet cells were absent in 1-week-old animals, emerged at 2-weeks of age and were highly populous in 3-week-old conjunctival tissue. MUC5AC is the major goblet cell secretory mucin, and our analysis showed that *Muc5ac* mRNA expression was highly upregulated in 3-week-old mice (Fig. 3c).

We found a large number of $CD11c^+$ and $CD11b^+$ cells with dendrites, presumably APCs, juxtaposing to the goblet cells in conjunctiva of 3-week-old mice (Fig. 3d). We speculated that these APCs may capture the antigens colonized in the conjunctival epithelium. In intestine, goblet cells establish so-called "goblet cell-associated antigen passages" (GAPs) in the second and third weeks after birth, which allow for the delivery of bacterial antigens from the intestinal lumen to the lamina propria[21]. Similar to the intestine, antigens bind to goblet cell secreted mucins in the conjunctiva and could be delivered to APCs via GAPs[22]. To determine the formation of GAPs during development in mice, we topically applied OVA, in the conjunctival sac at different time points from 2- to 4-weeks postnatally. Compared to 2- and 4-week-old mice, 3-week-old mice exhibited an increased migration of OVA from the conjunctival epithelium to the stroma, with partial uptake by APCs in the stromal area (Fig. 3e). We further examined the correlation between the ocular surface microbiome and conjunctival status using Mantel tests (Fig. S2). This revealed that the ocular microbial communities exhibit a significant correlation with *Muc5ac* mRNA expression, conjunctival epithelial layers and the number of goblet cells in 2-week-old mice. The conjunctival microbial communities in 3-week-old mice, moreover, exhibit a significant correlation with the percentage of deep intraepithelial APCs (Fig. S2). These results demonstrate that the conjunctival microbiome in neonatal mice helps enhance maturation of conjunctival development during eyelid-opening and supports the recruitment of APCs in ocular surface mucosa, which can be located in close proximity to goblet cells and extend trans-epithelial dendrites toward the ocular surface at 3-weeks of age to sample microbes via GAPs.

Disruption of the conjunctival microbiome in early postnatal life affects the maturation of conjunctival tissue

To determine whether early elimination of commensal microbiome would affect the maturation of conjunctival tissue, 0.3% tobramycin solution was applied to the murine ocular surface around the time of eyelid-opening, i.e, 2-weeks postnatally, and for 7 days thereafter (Fig. 4a). Bacterial culture of the conjunctival tissue from antibiotic-treated group mice (Tob) showed lower bacterial colonies compared with control-group saline-treated mice (Ctrl) after 7-days treatment (i.e., at the 3-week timepoint) (Fig. S3a). The subsequent profiling of the composition of the conjunctival microbiome by 16S rRNA gene sequencing (Table S1) revealed that, in comparison with the Ctrl group mice, Tob group mice had a significantly altered conjunctival microbiome after 7-days treatment (Fig. 4b). Changes were apparent in the composition and potential functions associated with cellular process and carbohydrate metabolism predicted by PICRUST2 (Fig. S3b).

Compared to control tissues, topical antibiotic exposure resulted in a reduction in the number of goblet cells in the murine conjunctiva (Fig. 4c) and a downregulation of *Muc5ac*, *Ki67*, and *Krt19* gene expression (Figs. 4c and S3d, e). The examination of GAPs indicated a reduction of OVA uptake in Tob group mice compared with mice in the control group (Fig. 4d). There was no evidence of apoptosis nor disruption of cell junctions during the experimental period (Fig. S3c, f). Meanwhile, to examine the effect of tobramycin on conjunctival cells, we excised conjunctival tissue from eyelid-opening mice and cultured extracted cells as previously described[23]. This revealed that all cells grow from the explants stained positively for Krt19, confirming their identity as conjunctival epithelium (Fig. S4a). Subsequently, the cells were cultured in media containing 0.03 mg/mL, 0.3 mg/mL, and 3 mg/mL tobramycin, respectively. Cell viability assays indicated no toxicity at any of the tested concentrations. Tobramycin, moreover, elicited no effect on the proliferation of the cultured cells (Fig. S4b). The number of $CD45^+$ cells in the conjunctival epithelium, however, were less in the conjunctivas of Tob group mice (Fig. 4e, f). Compared with Ctrl group mice, fewer MHC II positive cells and a lower

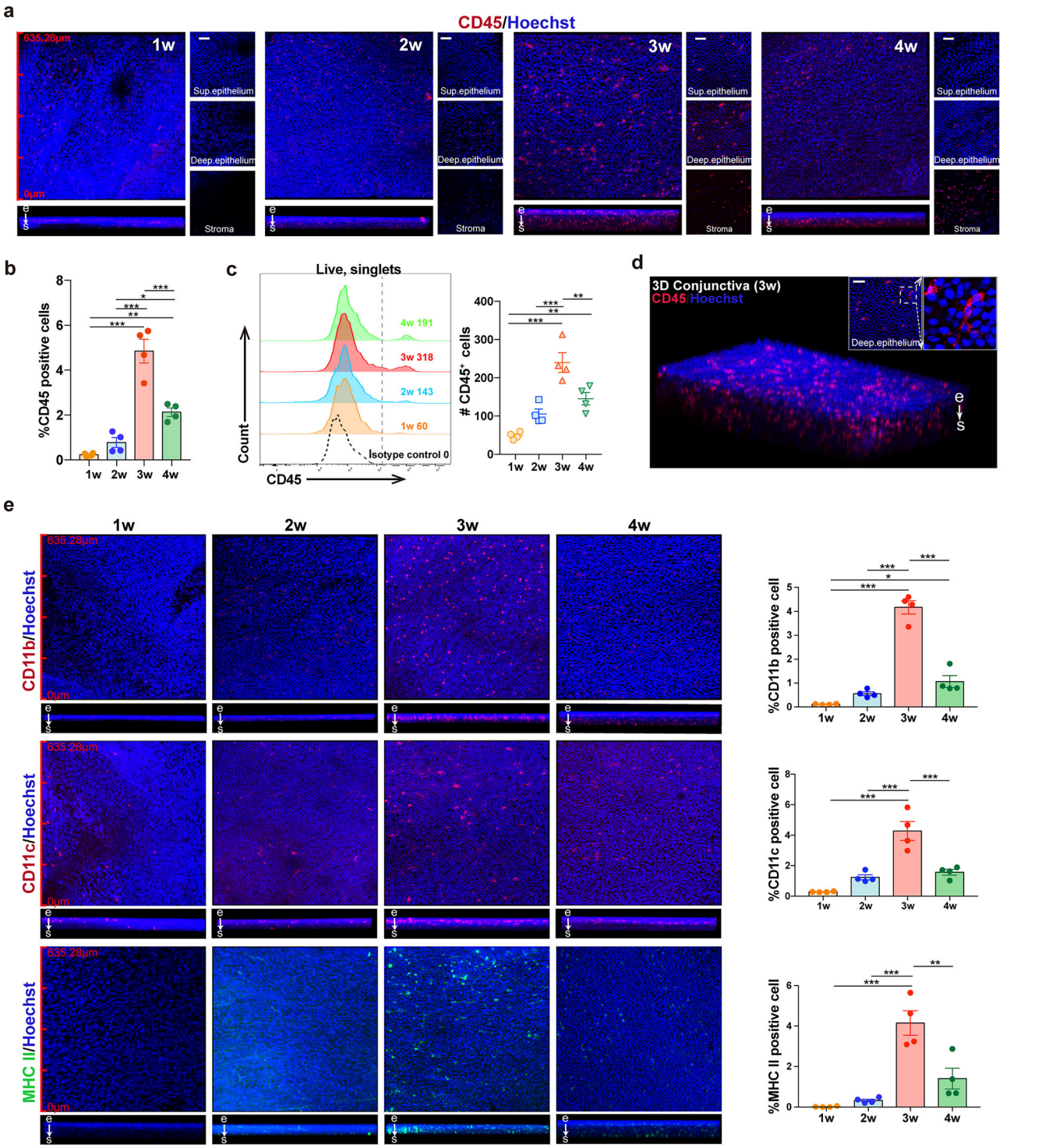

Fig. 2 | APCs are present in the conjunctival epithelium in 3-week-old mice. **a** Immunofluorescence wholemount staining of conjunctival tissue from 1-, 2-, 3-, and 4-week-old mice. Top left panels show surface view (×200 magnification); lower left panels show distribution of CD45 positive cells in the conjunctiva (using the Z-stack option) from the epithelium (e) to stroma (s). Smaller right panels are of superficial (Sup), deep epithelium and of stroma (×400 magnification). Representative images of three independent experiments. **b** The percentage of CD45 positive cells among conjunctival epithelium from 1-, 2-, 3-, and 4-week-old mice ($n = 4$ per group). **c** Representative histograms of staining for CD45 in live single-cell from the conjunctiva suspensions of 1-, 2-, 3-, and 4-week-old mice under steady-state conditions. Scatter plots present the counts of CD45 positive cells ($n = 4$ per group). **d** Laser confocal microscopy images of the conjunctival tissue from 3-week-old mice. Tissue was stained with monoclonal antibody (mAb) against CD45 (red) and with Hoechst dye (blue) for nuclear visualization (×200 magnification). Top right panel shows deep epithelium (×400 magnification). The white box in the deep epithelium image is shown to better illustrate immune cell processes. **e** Immunofluorescence staining of whole-mount fornix conjunctiva from 1-, 2-, 3-, and 4-week-old mice. Top panels show surface view (×200 magnification); lower panels show the distribution of CD11b, CD11c, and MHC II positive cells in the conjunctiva using the Z-stack option from epithelium (e) to stroma (s). The percentages of CD11b, CD11c, and MHC II positive cells among conjunctival epithelium from 1-, 2-, 3-, and 4-week-old mice ($n = 4$ per group). Scale bar, 50 μm. Data are shown as mean ± SEM. $^{*}P < 0.05$, $^{**}P < 0.01$, $^{***}P < 0.001$ using the one-way ANOVA.

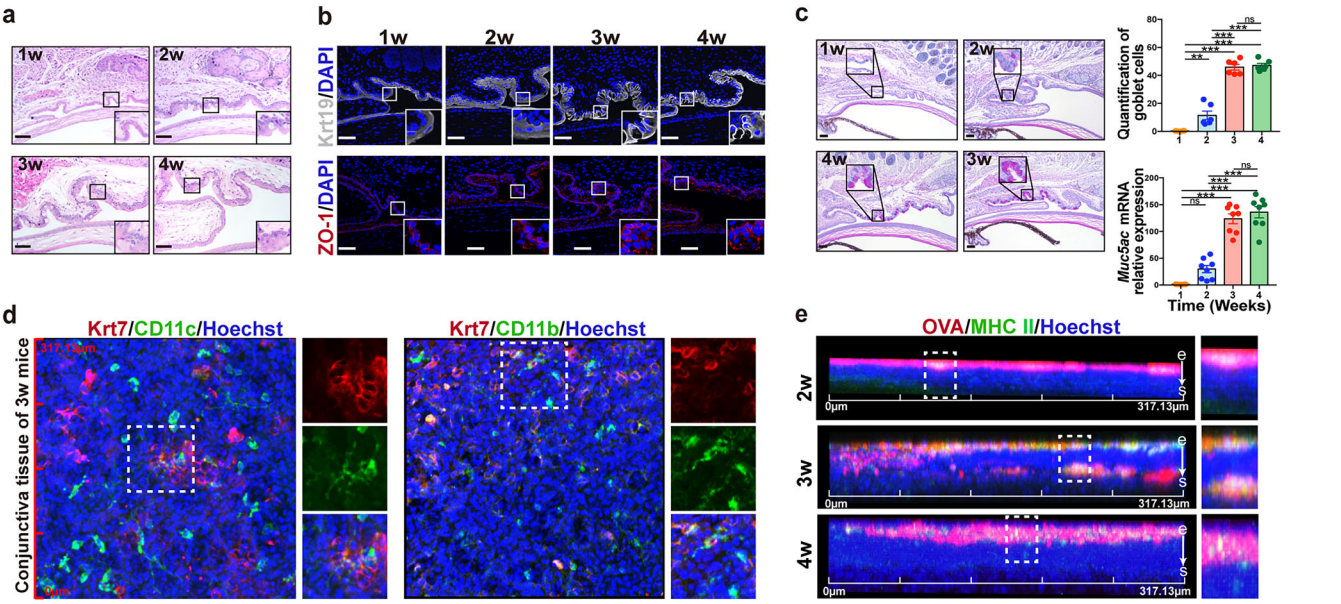

Fig. 3 | The conjunctival epithelial barrier is fully mature in mice at 3-weeks of age and cross-talk between APCs and antigens occurs via goblet cell associated passages (GAPs). a Representative image of H&E-stained sections of conjunctiva of 1-, 2-, 3-, and 4-week-old mice. **b** Immunofluorescence staining of conjunctival sections of 1-, 2-, 3-, and 4-week-old mice with monoclonal antibodies directed against cytokeratin 19 (Krt19, gray), ZO-1 (red) and DAPI (blue). **c** Representative images of conjunctival sections of 1-, 2-, 3-, and 4-week-old mice stained with PAS. The quantification of goblet cells and the *Muc5ac* mRNA expression in conjunctiva of 1-, 2-, 3-, and 4-week-old mice ($n = 6–8$ per group). **d** Immunofluorescence staining of whole-mount conjunctival tissue from 3-week-old mice stained for cytokeratin 7 (Krt7, red) and CD11c (left, green) or CD11b (right, green), with cell nuclei stained with Hoechst dye (blue) (×400 magnification). White box image is shown to better illustrate the location and morphology of CD11c and CD11b positive cells. **e** Z-stack option from epithelium (e) to stroma (s) showing the distribution of 45 kDa OVA (red) in three different growth stages 30 min after topical application to the ocular surface. White squares are magnified on the right. OVA uptake by APCs colocalizes with MHC II (green). Scale bars, 50 μm. Data are shown as mean ± SEM. ns $P > 0.05$, $^{**}P < 0.01$, $^{***}P < 0.001$ using the one-way ANOVA.

expression level of MHC II-related gene *H2-Ab1* was noted in the conjunctiva of Tob group mice (Fig. 4g). To assess whether this effect was direct, we performed an in vitro co-culture of mouse cervical lymph node (CLN) cells with tobramycin. We found that, except at the highest concentration (3 mg/mL), tobramycin at 0.03 mg/mL and 0.3 mg/mL showed no significant effect on MHC II expression in CLN cells (Fig. S4c). Together, these data support the notion of a local microbiome at the ocular surface that helps maintain ocular mucosal homeostasis, and that the transient disruption of the microbiome via antibiotics in the week following eyelid-opening may delay conjunctival maturation and disequilibrate ocular mucosal homeostasis.

Longer-term effects of early postnatal antibiotic exposure on ocular surface mucosa

To investigate the longer-term effect on conjunctival tissue of disruption of the ocular surface microbiome by topical antibiotic exposure following eyelid-opening, the microbial composition characteristics of the conjunctiva were surveyed by 16S rRNA gene sequencing 1-week (i.e., mice at 4-weeks of age) or 2-weeks (i.e., 5-week-old mice) after the cessation of tobramycin/saline application for 7-days, which started at 2-weeks of age (Table S1). This analysis indicated that the effect of topical antibiotic exposure on the composition of the microbiome was still evident 2 weeks (i.e., in 5-week-old mice) after discontinued antibiotic application (Fig. 4b). At 4- and 5-weeks of age, there were significant differences in β-diversity between Ctrl and Tob groups (Fig. 5a). We further explored the bacterial co-occurrence patterns and found that there was an obvious ecological network difference between the Ctrl and Tob groups in both 4-week and 5-week mice (Fig. 5b and Table S4). Additionally, compared with Ctrl group mice, Tob group mice at 4 weeks had significantly higher Shannon and Simpson indices, however, there were no significant differences in α-diversity between the groups at 5-weeks of age (Fig. S5a). We also used PICRUSt2 to predict the functions of the microbiome in each group, which showed that in Tob group mice the microbiome pointed to a substantially different potential functions compared with Ctrl group mice at 4 weeks of age (Fig. S5b). This was not the case at 5 weeks, however, with Tob vs Ctrl groups showing smaller difference. Together, the data suggest that the diversity and potential functions of conjunctival microbiome are gradually recovering 2 weeks after discontinued topical antibiotic exposure that started during eyelid-opening, even though composition of conjunctival microbiome remained unrestored.

Conjunctival tissue from the experimental mice was examined, which disclosed that the number of conjunctival goblet cells and levels of mucin secretion and Krt19 expression had been restored at 4 weeks (Fig. S5c, d), but MHC II positive cell numbers were higher in Tob group mice at 4 and 5 weeks compared to numbers in Ctrl group mice (Fig. 5c). Additionally, conjunctival immune reactivity to antigens by topically applied OVA (45KD) 30 min before euthanasia revealed a significant increase in the frequency of intraepithelial $CD11b^+$ cells in the conjunctiva of Tob group mice at 4- and 5-weeks of age compared to mice in the Ctrl group at these junctures (Fig. 5d). This indicates that early antibiotic exposure after eyelid-opening may have an extended effect on the colonization of the conjunctival microbiome and may impair tolerance to environmental exposures, eventually leading to a potential aggravation of the response of $CD11b^+$ cells to antigens in the conjunctiva of mice.

Absence of the conjunctival microbiome in early postnatal life exacerbates the ocular allergic response

Postnatal exposure to bacteria and their products helps modulate the development of the immune system, and these influences may be durable[14]. If the communication between host and microbiome is disturbed in early postnatal life, excessive immune reactivity may develop in adulthood, which can lead to increased susceptibility to allergic diseases[24]. Because the conjunctiva-commensal relationship was formed during eyelid-opening, we hypothesized that disruption of ocular surface microbiome in this period would lead to an aggravation of allergic eye disease (AED). To investigate that we studied unimmunized control mice (naive), AED mice by OVA

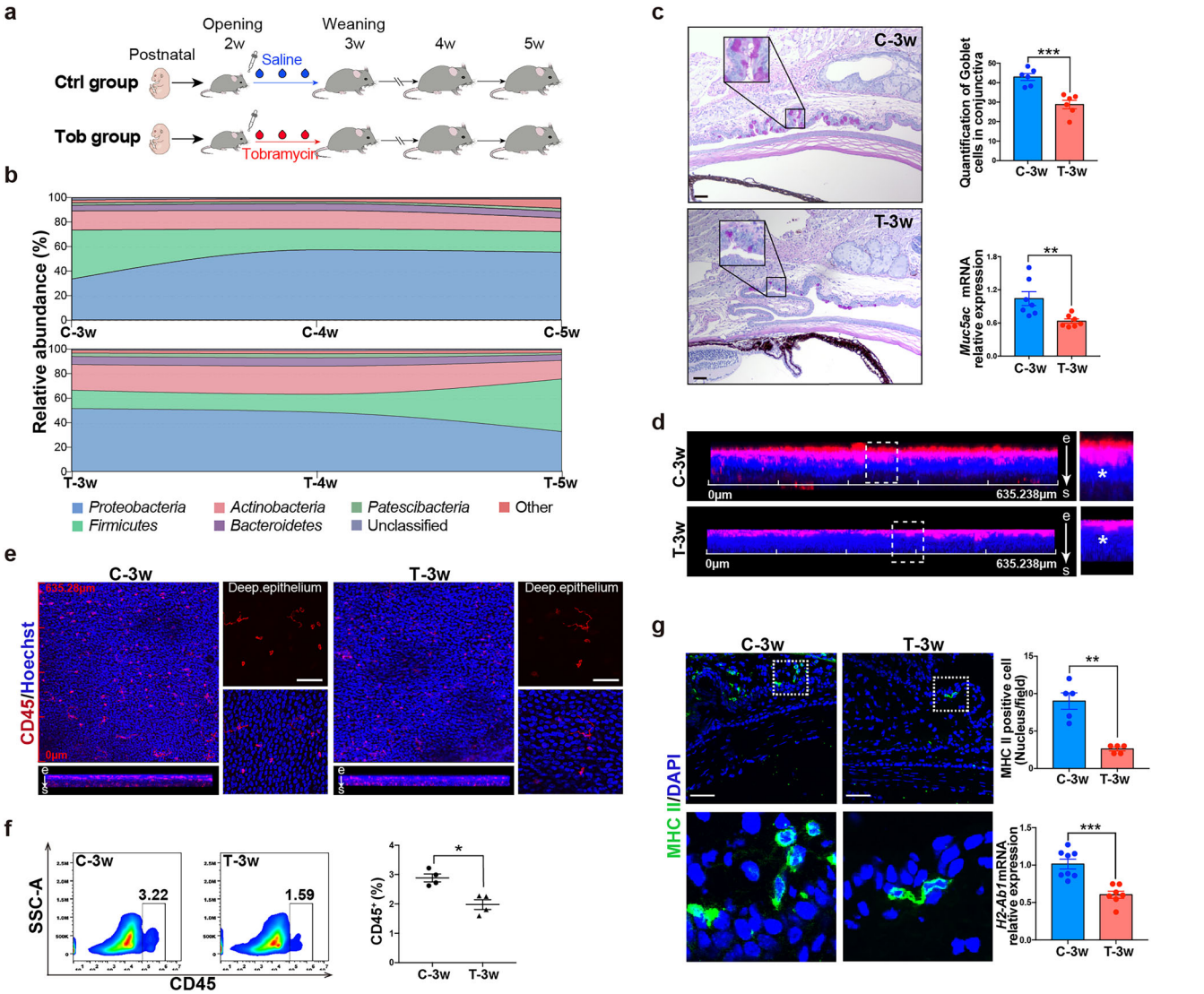

Fig. 4 | Topical antibiotic exposure in early postnatal life leads to changes in the composition of the conjunctival microbiome and disrupts mucosal homeostasis. **a** Study design of topical antibiotic exposure in early postnatal life. **b** Composition of the microbiome in saline-treated group mice (Ctrl) and antibiotic-treated group mice (Tob) at specific intervals after the discontinuation of 1-week's application of topical antibiotics that ended at the 3-week timepoint. ($n = 10$ per group). **c** Representative images of conjunctiva sections of 3-week-old Ctrl group mice (C-3w) and Tob group mice (T-3w) stained with PAS. The quantification of goblet cells ($n = 6$ per group) and the *Muc5ac* mRNA expression ($n = 7$ per group) in the conjunctiva of C-3w and T-3w mice. **d** GAPs (columns) were identified (asterisks) of whole-mount conjunctival tissues from C-3w and T-3w mice (×200 magnification). White squares are magnified on the right. **e** Immunofluorescence staining of whole-mount conjunctival tissue from C-3w and T-3w mice with CD45 (red) and cell nuclei stained with Hoechst dye (blue) (×200 magnification). Lower left panels show the distribution of CD45 positive cells in the conjunctiva using Z-stack option from the epithelium (e) to stroma (s). Smaller right panels are of deep epithelium. Representative image of three independent experiments. **f** Flow plots of staining for CD45 in conjunctival single-cell suspensions from the conjunctival tissues from C-3w and T-3w mice. Scatter plots present the percentages of CD45-positive cells in the conjunctival tissues of C-3w and T-3w mice ($n = 4$ per group). **g** Immunofluorescence of conjunctival sections from C-3w and T-3w mice with monoclonal antibodies against MHC II (green) and DAPI (blue). White squares are magnified on the bottom. The quantification of MHC II positive cells ($n = 5$ per group) and the MHC II-related gene *H2-Ab1* mRNA expression in the conjunctiva of C-3w and T-3w mice ($n = 8$ per group). Scale bars, 50 μm. Data are shown as mean ± SEM. $^{*}P < 0.05$, $^{**}P < 0.01$, $^{***}P < 0.001$ using unpaired t test and Mann–Whitney U test.

administration and antibiotic-treated AED mice (Tob+OVA) (Fig. 6a). The data indicated that compared with naive mice, OVA mice developed a significant allergic response, whilst Tob+OVA mice presented with even more severe clinical manifestations (Fig. 6b), with higher clinical scores (Fig. 6c) and elevated serum IgE levels (Fig. 6d). The number of eosinophils infiltrated in the conjunctiva was prominently increased in Tob+OVA mice compared to the naive and OVA mice when determined by Picrosirius Red staining (Fig. 6e). The results of toluidine blue staining, a useful method to recognize mast cells and evaluate degranulation, revealed a significant increase in mast cell numbers in the conjunctiva of Tob+OVA mice compared to naive and OVA mice (Fig. 6f). We imaged freshly excised mouse conjunctival tissues based on a moxifloxacin-based fluorescence imaging method and discovered that, compared with naive mice, the number and density of goblet cells and *Muc5ac* mRNA expression were significantly increased in OVA mice, and were more prominent in antibiotic-treated AED mice (Fig. 6g). Furthermore, antibiotic treatment significantly increased the number of MHC II^{+} cells and $CD4^{+}$ T cells in conjunctiva of AED mice. The mRNA expression levels of the transcription factor *Gata3* in Th2 cells, along with the cytokines *IL-4* and *IL-5* secreted by these cells, exhibit a substantial increase in conjunctiva of antibiotic-treated AED mice (Fig. 6h). Given that secondary T helper cell responses generated in the lymph node are responsible for causing AED, as previously

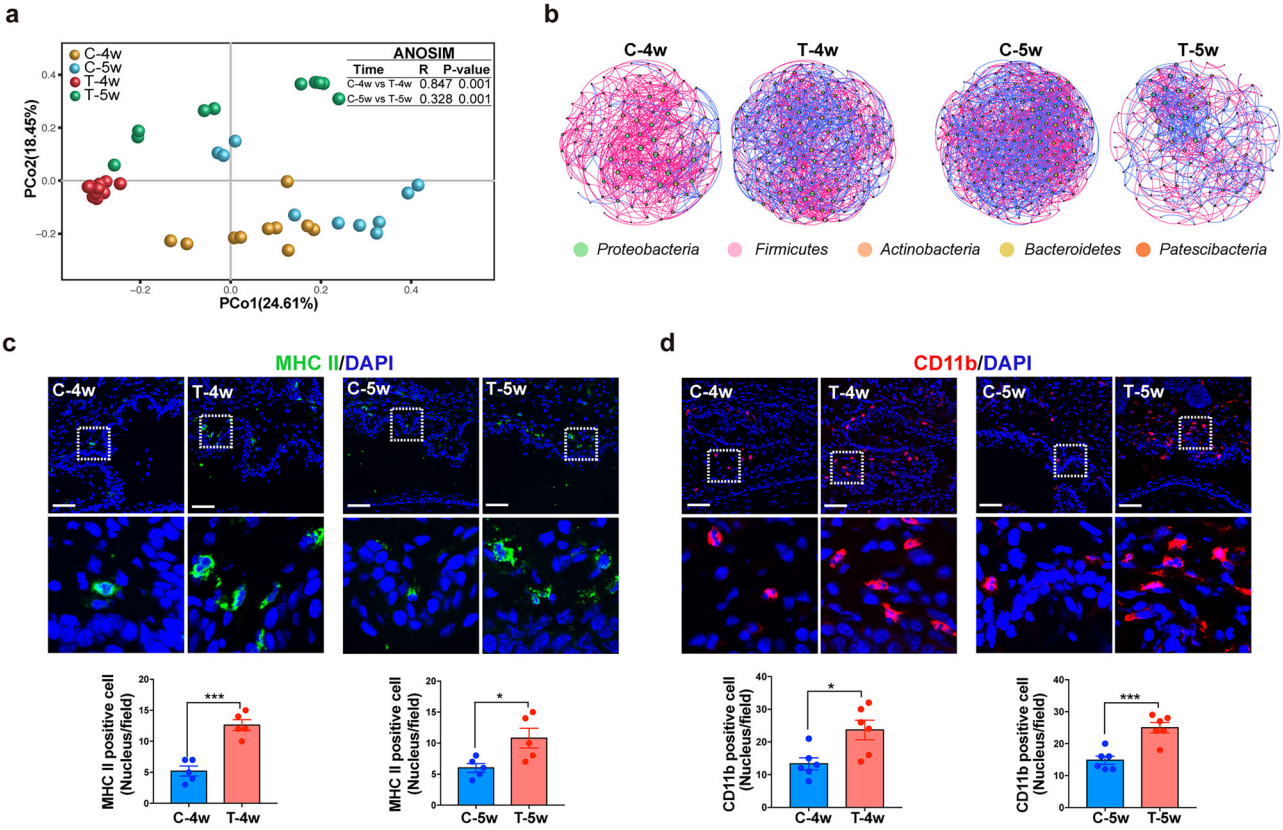

Fig. 5 | Topical antibiotic exposure in early postnatal life leads to longer-term effects on microbial colonization and ocular mucosal homeostasis. a Principal coordinate analysis plot generated using OTU metrics based on the Bray-Curtis dissimilarities. Each point represents a sample. **b** The networks of co-occurring bacterial OTUs in conjunctiva of the groups after discontinued antibiotic/saline application for 1 week (C-4w, T-4w) and 2 weeks (C-5w, T-5w) based on the correlation analysis. The co-occurring networks are colored by phylum. A red edge indicates a positive interaction between two individual nodes, while a blue edge indicates a negative interaction. **c** Immunofluorescence of conjunctival sections of the groups which discontinued antibiotic/saline application for 1 week (C-4w, T-4w) and 2 weeks (C-5w, T-5w) with monoclonal antibodies against MHC II (green) and DAPI (blue). White squares are magnified on the bottom. The quantification of MHC II positive cells of conjunctiva in the Ctrl and Tob groups at 4 weeks and 5 weeks ($n = 5$ per group). **d** Immunofluorescence of conjunctival sections in the Ctrl and Tob groups at 4 and 5 weeks, in mice which had received topically applied OVA (45 KD) 30 min before euthanasia. Monoclonal antibodies are directed against CD11b (red) and DAPI (blue). White squares are magnified on the bottom. The quantification of CD11b positive cells in conjunctiva in the Ctrl and Tob groups at 4-and 5-week mice ($n = 6$ per group). Scale bars, 50 μm. Data are shown as mean ± SEM. $^{*}P < 0.05$, $^{***}P < 0.001$ using the unpaired t test.

described[25], we further examined T cell subsets in CLN of mice from different group. Flow cytometry analysis revealed that, compared to the naive mice, OVA mice exhibited a significant increase in the frequency of Th1 ($CD4^+$ IFN-γ^+) and Th2 ($CD4^+$ IL-4^+) cells in the CLN cells, accompanied by a significant decrease in the frequency of Treg ($CD4^+$ $CD25^+$ $Foxp3^+$) cells. Notably, in Tob+OVA mice, the Th2 response was further elevated, accompanied by a lower frequency of Treg cells compared to OVA mice (Fig. 7a–c).

The same approach (Fig. S6a) was used to examine if the topical antibiotic treatment for 7 days of weaning (3-weeks-old) or adult (6-weeks-old) mice would similarly aggravate AED, which indicated that both Ctrl and Tob groups showed comparable increases in allergic manifestations (Fig. S6b, c) and possessed equivalent numbers of eosinophilic and mast cells (Fig. S6d, e). Consistent with the above findings, antibiotic treatment did not alter the number of $CD4^+$ T cells nor the mRNA expression levels of *Gata3*, *IL-4*, and *IL-5* (Fig. S6f). These results suggest that, compared with Ctrl group mice, AED is not aggravated in either weaning or adult Tob group mice. Collectively, these findings highlight the potential impact of perturbations to the cross-talk between the host and conjunctival microbiome in early postnatal life on the aggravation of AED.

Discussion

This study characterizes the dynamic changes of the ocular surface microbiome during postnatal development in mice. We observed that the phyla *Proteobacteria* and *Firmicutes* dominate the ocular surface microbiome at different postnatal stages in murine conjunctiva, and these two dominant phyla have also been found in the conjunctiva of children[5,26]. Unlike in humans, however, mouse eyelids remain closed during early postnatal life and open about 2 weeks after birth. Due to the diminutive size of mice eyes and the relatively low microbial load, sustained observations over time in individual eyes are unfeasible, thus, we chose to study tissue excised at different ages from eye opening through to maturity. We also note that knowledge of the ocular surface microbiome in humans comes from investigations of children of different age groups[4,5,27], and that there is a need for a more comprehensive scrutiny of ocular surface microorganisms in humans from the neonatal stage to adulthood. In this study, we found that the murine ocular surface microbiome changed significantly during eyelid-opening, allowing us to conclude that external factors have a critical impact on the ocular surface microbiome of mice. In humans, it is likely that the mode of delivery and external influences may have a significant impact on the ocular surface microbiome of newborns. The most common conjunctival bacteria are coagulase-negative Staphylococcus accompanied by bacteria characteristic of vaginal flora in the conjunctiva of infants delivered vaginally compared those born via C-section delivery[28,29]. Additionally, the composition of the ocular surface microbiome underwent changes subsequent to antibiotic prophylaxis involving gentamicin in newborns[4]. This outcome parallels our observations in mice. Compared to other factors, the composition of the ocular surface microbiota is less influenced by gender,

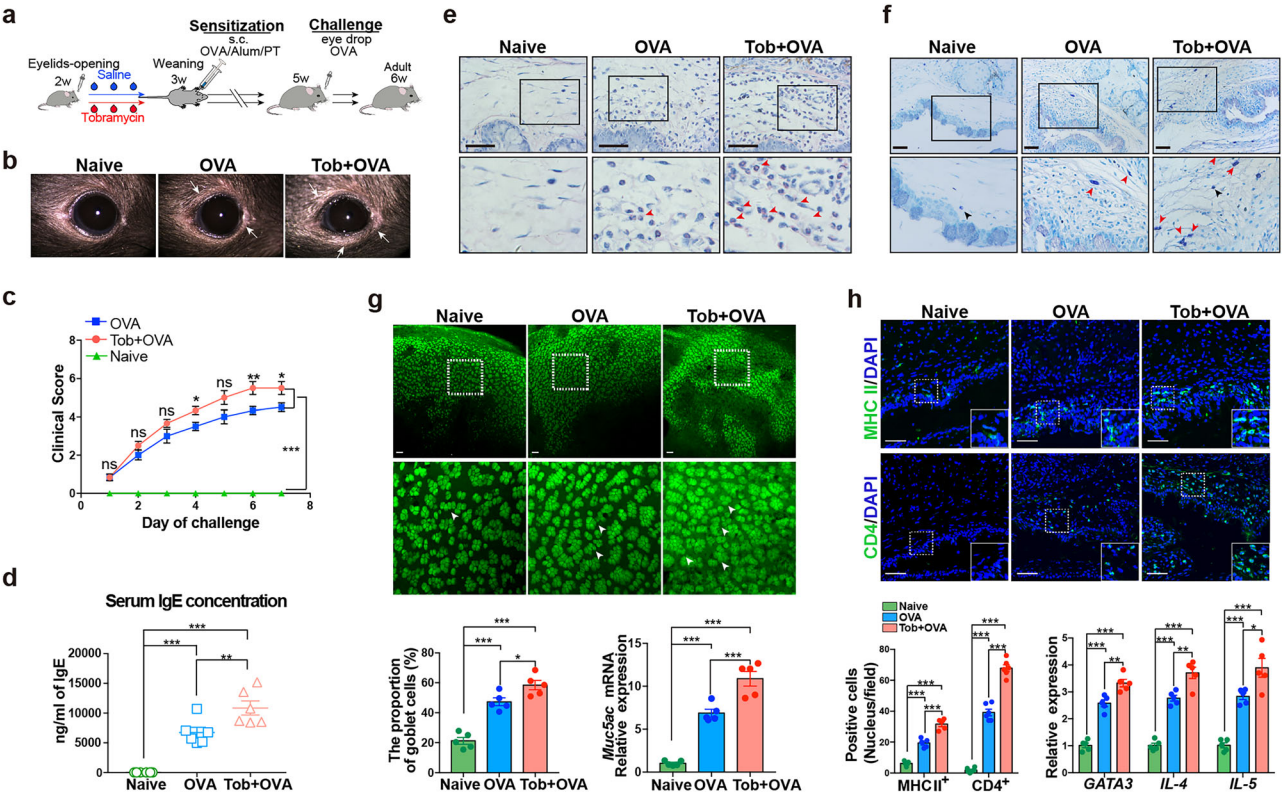

Fig. 6 | Disruption of the conjunctival microbiome in early postnatal life exacerbates the development of allergic eye disease (AED). a Study design for inducting AED model after 1 week of topical antibiotic exposure in eyelid-opening mice. **b** Clinical manifestations such as blepharitis (white arrows) and clinical scores were assessed. **c** Scoring was performed 20 min post challenge based on four independent parameters, which include lid edema, tearing/discharge, chemosis and hyperemia. Each parameter was ascribed 0 to 3+ points and were summed to yield a maximum score of 12+ ($n = 6$ per group). **d** Blood was collected and the serum IgE levels assessed via ELISA. The concentration of IgE in mice serum ($n = 6$ per group). **e** Eosinophilic infiltration. Black squares are magnified on the bottom. Red arrows indicate eosinophils. **f** Mast cells (MCs) were stained by toluidine blue, with normal MCs identified based on their regular shape (black arrows) and activated MCs identified based on their irregular shape (red arrows) in conjunctivas of unimmunized control mice (naive), AED mice (OVA) and topical antibiotic exposure AED mice (Tob+OVA) in early postnatal life. **g** Moxifloxacin-based confocal microscope images of conjunctival tissue. White squares are magnified on the bottom. Clusters of highly fluorescent and reflective cells are marked with white arrows. The proportion of goblet cells and the *Muc5ac* mRNA expression in conjunctival tissues in conjunctiva in naive, OVA and TOB + OVA groups ($n = 5$ per group). **h** Immunofluorescence of conjunctival sections in naive, OVA and TOB + OVA groups with monoclonal antibodies against MHC II (green), CD4 (green) and DAPI (blue). The quantification of CD4 and the MHC II positive cells in conjunctiva of naive, OVA and TOB + OVA groups ($n = 5$–6 per group). The *Gata3*, *IL-4*, and *IL-5* mRNA expression in conjunctiva of naive, OVA and TOB + OVA groups ($n = 6$ per group). Scale bars, 50 μm. Data are shown as mean ± SEM. ns $P > 0.05$, $^{*}P < 0.05$, $^{**}P < 0.01$, $^{***}P < 0.001$ using the one-way ANOVA.

consistent with findings in humans[30], with male and female mice found to differ only in the β-diversity of the conjunctival microbiome.

In other sites in newborn infants, such as the skin, gut and oral cavity, the initial microbiota evolves over time and adapts to the physiological variation[31,32]. The current data support the concept of a gradual adaption of the conjunctival microbiome in 4-week-old mice to 8-week-old mice, which may be a result of host adaptation and interaction with the environment. Specifically, factors such as the enhanced barrier function of the ocular surface epithelial cells, increased release of the antibacterial components in the tear fluid, and the maturation of the ocular mucosal immune system may influence the pattern of microbial colonization. Concurrently, the behavioral changes in mice, such as grooming, solid food intake and exploration, may affect the contact of ocular surface with environmental microbes. This expanded environmental exposure may promote the colonization and selection of diverse microbial communities, thereby contributing to the gradual stabilization and maturation of the conjunctival microbiome. Intriguingly, microbial presence was also detected in the conjunctiva of 1-week-old postnatal mice, even when the eyelids were still closed. Given the extremely low microbial biomass in conjunctival tissues at this stage, the possibility of trace contamination cannot be completely excluded. However, several measures were taken to minimize the risk of contamination, including sterile dissection procedure and collection of negative controls. Further analysis showed that the microbial relative abundance in the negative controls was significant lower, although these controls did reveal a variety of potential contaminants identified in prior study[33]. Furthermore, a significant distinction in the microbial composition was evident between the conjunctival microbiome and negative controls. Therefore, the microbial signals detected in conjunctiva of 1-week-old postnatal mice may not be from contamination. Meanwhile, we conducted additional filtration based on the IndVal index to address potential contaminations in the conjunctival microbiome. Following filtration, multiple dominant genera still persist in the conjunctival tissues derived from 1-week-old mice, which may be due to the nature of the developmental process of the mouse eye in utero[34], rather than being indicative of potential contamination. However, the origin of the pre-eye-opening ocular microbiome in mice is currently unestablished and ocular mucosa-microbial interactions before eye opening in mice needs further exploration.

Microbial cohabitants are major participants in shaping and maintaining essential physiological processes[35]. The conjunctiva is colonized by a unique commensal microbiome, and like the skin, these commensal communities stimulate and educate defense and immune responses[36], which contribute to the development of symbiosis between the host and microbiome. Such symbiotic relationships depend on early events taking place during perinatal life[37]. Our results suggest that

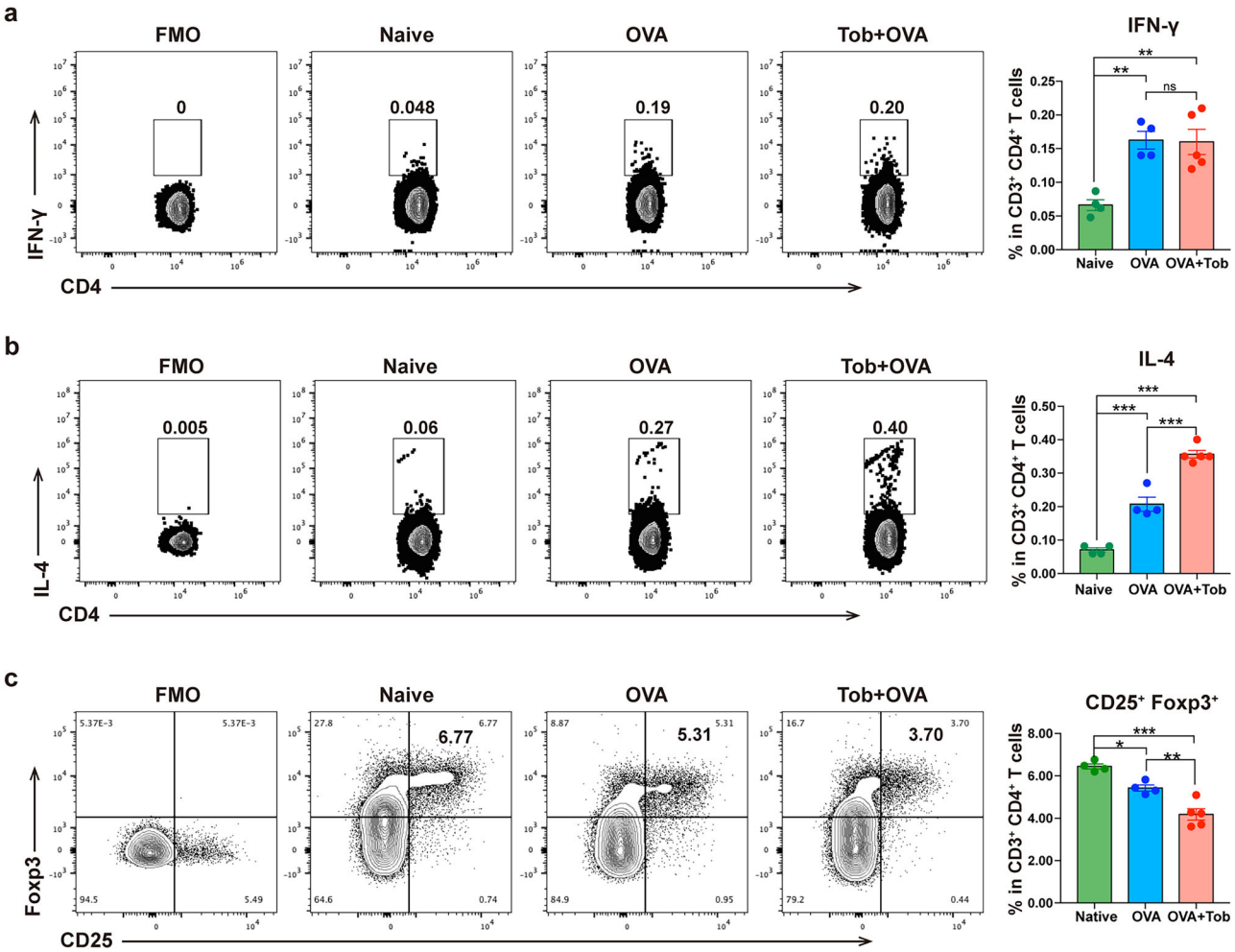

Fig. 7 | Th2 and Treg cell frequencies in the draining lymph node of AED mice are affected by topical antibiotic exposure in early postnatal life. The frequency of Th1 ($CD4^+$ IFN-γ^+) (**a**), Th2 ($CD4^+$ IL-4^+) (**b**) and Treg ($CD4^+$ $CD25^+$ $Foxp3^+$) cells (**c**) in CLNs of naive, OVA and Tob+OVA groups ($n = 4$–5 per group). Data are shown as mean ± SEM. ns $P > 0.05$, $^*P < 0.05$, $^{**}P < 0.01$, $^{***}P < 0.001$ using the one-way ANOVA.

postnatal conjunctival barrier maturation and immune responses accompany the dynamic changes of commensal microbiome and that these include conjunctival epithelial cell stratification, goblet cell development, mucin secretion and temporary recruitment of APCs into the conjunctival epithelium. Notably, in 3-week-old mice, BugBase analysis predicted a higher relative abundance of potential pathogenic bacteria in the conjunctiva compared to other developmental stages, with significant alterations observed in genera such as *Enterococcus*, *Staphylococcus*, and *Sphingobacterium*. This period also coincided with a peak in immune activation. Despite the presence of multiple known opportunistic pathogens within these genera, their increased abundance at this stage did not induce any significant pathological changes. Previous studies suggest that, at appropriate levels, certain opportunistic bacteria may contribute the establishment of host–microbe symbiosis and even play beneficial roles in immune system development[38]. The massive influx of microbes and microbial antigens greatly influences the expansion and differentiation of a variety of different cell types[39]. In both humans and mice, colonization by commensal flora during early life can drive differentiation of Treg cell, thereby suppressing inflammation[40,41]. In our study, the heightened immune activation at 3 weeks, followed by its reduction at 4 weeks, may be due to Treg-mediated immune regulation during this critical postnatal period. It is noteworthy that, although our data suggest an association between postnatal conjunctival barrier maturation, immune response and conjunctival microbial colonization, direct evidence of a causative relationship is lacking. Therefore, future studies using germ-free mouse are essential to determine the effects of microbial colonization on the development of the ocular mucosal immune system.

Conjunctival goblet cells are located at the interface between the external environment and stromal immune cells, which allows them to easily convey information between the external antigen and the APCs. Meanwhile, the goblet cell products presumably modulate APC function in maintaining immunological tolerance on the ocular surface[42,43]. In support of this, we note that extensions of dendritic cells surrounding goblet cells project across the epithelium towards the ocular surface in the conjunctiva of $TSP1^{-/-}$ mice, which are reported to harbor increased microbial frequency at the ocular surface[44]. We also found a significant increase in the number of APCs in the conjunctival epithelium of 3-week-old mice, and extensions adjacent to goblet cells demonstrated ability of ocular mucosal APCs to extend trans-epithelial dendrites in response to sudden bacterial colonization at the ocular surface. In addition, conjunctival goblet cells responding to TLR signaling[44], epithelial cell-derived cytokines and chemokines[45,46], as well as neuropeptides signaling[47], may also contribute to this process. Such interactions may facilitate tolerance to environmental exposure during eyelid-opening, although further studies will be needed to incorporate FISH for a more comprehensive assessment of bacterial localization in conjunctiva and to establish the mechanism by which microbes promote ocular surface immune tolerance during early postnatal life. Furthermore, GAPs are considered a route for antigen delivery to APCs[22]. We observed an increased distribution of OVA in the conjunctival stroma of

3 weeks of age, with partial uptake by APCs. However, OVA antigen delivery to the stromal area were reduced despite the continued presence of GAPs in 4-week-old mice. This phenomenon may be influenced by multiple regulatory pathways, including microbial, immune and neurotransmitter signaling[21,48,49].

After birth, bacterial colonization of mucosa plays critical roles in the development and education of the host mammalian immune system[50]. This period is termed the "window of opportunity" and if there is an absence of appropriate microbial exposure, the immune consequences may elicit irreversible and potentially deleterious implications for the host including inflammatory bowel disease[16], allergy[51,52] and asthma[15]. The "window of opportunity" may also exist at other mucosal surfaces, and in this study, we report that when the eyes 2-week-old open and are treated with antibiotics for 1 week, the ocular surface microbiome is significantly altered, with an inhibition of goblet cell development and immune cell recruitment. Simultaneously, in vitro cell experiments revealed that 0.3% tobramycin exhibited no anti-proliferation effect on conjunctival epithelial cells following a 24-h incubation. In the gut, symbionts play an indispensable role for intestinal stem cell-mediated epithelial development, the use of lactic-acid-producing bacteria type symbionts can significantly increase the expansion of intestinal stem cells, Paneth cells and goblet cells in mice[53]. Therefore, these findings substantiate that the delayed maturation of the conjunctiva may result from antibiotic-mediated elimination of the conjunctival microbiome rather than a direct impact on conjunctival epithelial cells, and we note that conjunctival goblet cell reduction has also been found in germ-free mice[54].

Antibiotic exposure in early life may have long-term effects on microbial colonization. For example, in murine gut, microbiome may take at least 13 weeks to recover following antibiotic disruption[55], whereas the ocular surface microbiome in rabbits often returns within a few weeks after cessation of treatment[56]. The changes of microbiome induced by antibiotics, and the time required to restore to age-matched microbial composition, depend not only on antibiotic clearance but also on microbial colonization dynamics and the immune status of the host[57,58]. Although the conjunctival microbiome composition in antibiotic-treated mice still differed from that of controls, we observed a trend toward recovery of the conjunctival microbiome two weeks after cessation of antibiotic exposure. The changes may be attributed to early antibiotic exposure, which can disrupt the interaction between the conjunctival microbiome and the ocular mucosal immune system, thereby altering mucosal immune homeostasis and delaying the re-establishment of environmentally driven commensal communities. Notably, despite the partial microbial recovery, the immune response to antigens in the conjunctiva remained changed, manifested as an increased response to antigens and aggravated AED. This was not the case in other period mice, however, indicating that there may be a similar "window of opportunity" with regards to the ocular surface, in which exposure to microbes appears critical to ensure proper conjunctival maturation that in-turn leads to conjunctival mucosal immunity and the prevention of susceptibility to allergic responses in adulthood.

Antibiotic treatment during early life has been linked to allergy development[59,60]. Although, the exact mechanisms are not fully elucidated, sufficient microbial exposure during early life appears essential for the development of healthy immune system. In humans and mice, neonatal $CD4^+$ T cells are biased towards Th2-type responses. Microbial exposure has been suggested to modulate this bias through the induction of Th1-type pathways or expansion of Treg cells, thereby promoting immune balance[61]. However, antibiotic exposure in early life reduces microbial stimulation, promoting a shift toward Th2 polarization and contributing to the development of allergic diseases[62,63]. In this study, early postnatal disruption of microbiome by antibiotic did not affect the AED-induced Th1 response. However, it exacerbated the Th2 response and further reduced Treg cell frequency, indicating that early-life microbial disruption may aggravate Th2-skewed immunity and impact Treg development or maintenance. Additional studies are needed to elucidate the mechanisms by which early-life crosstalk between the host and the conjunctival microbiome contributes to the exacerbation of AED.

AED impacts 10–20% of the population, exerting a significant negative impact on the ocular surface health and quality of life. Notably, among children, the highest prevalence occurs between 3 and 11 years of age[64]. The World Allergy Organization is raising awareness about the escalating burden of allergic diseases globally, particularly in children and developing countries[65]. Microbiological disruption may serve as a contributing factor to this phenomenon[66], a proposition supported by our research findings. Furthermore, during the establishment of AED in mice at various ages, we observed variations in the severity of the disease. Specifically, the allergic response in adult mice was notably more intense, possibly attributed to the mature immune development in adult mice and their heightened responsiveness to external allergens. Therefore, further investigation is warranted to explore the correlation between age and the severity of AED.

In summary, the colonization of microbiota in early life is crucial to the timely maturation of conjunctival mucosa and the establishment of ocular surface homeostasis (Fig. 8). The use of antibiotics in newborns may lead to a delayed ocular mucosal development and maturation of conjunctival mucosal immunity. If the cross-talk between the microbiome and conjunctival mucosa during early postnatal life is disrupted, delayed conjunctival maturation processes could aggravate the subsequent development of allergic eye disease. Therefore, the application of antibiotic eye drops in newborn infants should be more carefully considered and the established neonate ocular prophylaxis policy throughout the world may need to be revisited.

Methods

Animal breeding and selection

C57 black 6 (C57BL/6J) mice comprise one of the most common inbred strains of laboratory mice. In this study, C57BL/6J mice were chosen to investigate the changes in the composition of the ocular surface microbiome and the immunology and functional events taking place in the conjunctiva from postnatal week-1 onward to adulthood at 8-weeks of age. All the animals used in this study were bred in the animal facility of Xiamen University Laboratory Animal Center (Xiamen, China). Initially, monogamous breeding pairs were purchased from Xiamen University Laboratory Animal Center and used through in-breeding. Post-birth, the pups were primarily fed on breast milk until the age of 3 weeks, then the animals were randomly separated into individual cages (5 mice per cage) at the age of 3–4 weeks. At the specified age, healthy non-littermates were randomly picked from the breeding pairs and divided into females and males. Mice were maintained in a standard pathogen-free environment at 25 ± 1 °C with a relative humidity of 60 ± 10% and a 12-h light-dark cycle (from 8:00 a.m. to 8:00 p.m.). The mice were fed ad libitum feed and autoclaved water. Experimental protocols were in accordance with the Association for Research in Vision and Ophthalmology's Statement for the Use of Animals in Ophthalmic and Vision Research and were approved by the Experimental Animal Ethics Committee of Xiamen University (XMULAC20170014). We have complied with all relevant ethical regulations for animal use.

Sample description

To explore the changes in the composition of the ocular surface microbiome during development, after the mice euthanized by cervical dislocation, conjunctival tissue samples were isolated from 40 C57BL/6J mice (80 eyes) at the age of 1 week, 2 weeks, 3 weeks, 4 weeks, 6 weeks, and 8 weeks under aseptic conditions, respectively. The dissection process was undertaken under sterilized conditions to avoid contamination. At each time point, 80 conjunctival tissue samples were collected and immediately frozen at −80 °C until further processing. Conjunctival tissue samples from 8 eyes were pooled as a single research sample, resulting in a total of 10 research samples per time point, comprising 5 samples from males and 5 from females. To address the challenges posed by contamination aligned to inefficiencies in microbiome analyses of low-biomass samples[67], at each sample collection event we collected laboratory environmental samples using a sterile swab exposed to the surrounding environment. These served as negative controls. Furthermore, feces samples in bedding were collected

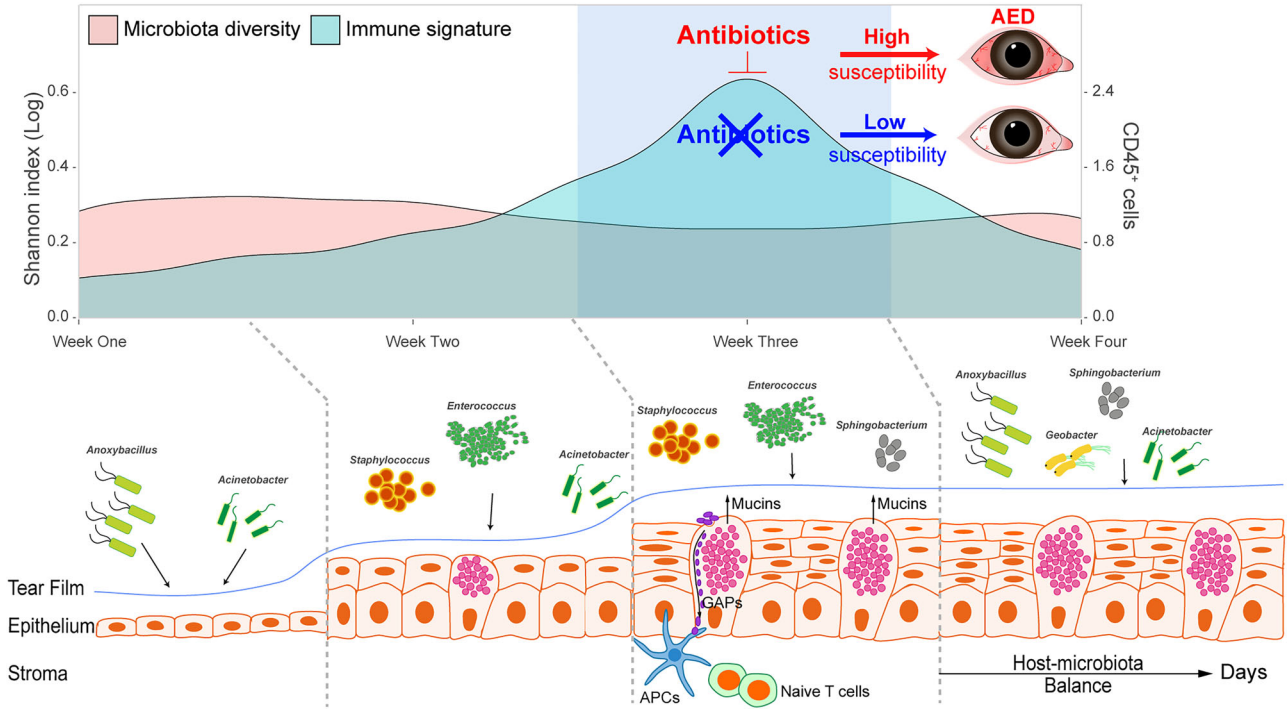

Fig. 8 | Summary schematic. The instantaneous microbial influx in early postnatal life induces the recruitment of APCs to the conjunctival epithelium and activates cross-talk between APCs and antigens via GAPs. Topical antibiotic exposure in early postnatal life disrupts mucosal homeostasis and leads to the ocular surface to become more susceptible to AED.

at the sampling time points and stored as described above to analyze the "environmental microbiome".

Antibiotic treatment

Tobramycin (Sangon Biotech, Shanghai, China) was dissolved in saline to make 0.3% tobramycin solution under sterile conditions. 2.5 µl of 0.3% tobramycin solution was applied to each eye of 2-week-old C57BL/6J mice three times daily. The control group received saline solution. Mice received the antibiotic/saline for 7 days until they were 3-week-old, at which time antibiotic/saline use was discontinued. The mice were euthanized by cervical dislocation at 3-, 4-, and 5-weeks of age. The conjunctival tissue sample collection at each time point was consistent with the descriptions above.

Induction of allergic eye disease (AED) model

Mice were immunized with a subcutaneous injection of 100 µg ovalbumin (OVA, InvivoGen, vac-stova), 300 ng pertussis toxin (Abcam, ab124299) and 1 mg aluminum hydroxide (Acmec, A19200) in 100 µl PBS. After 2 weeks, mice were challenged once/day with 5 µl OVA (50 mg/ml) in PBS, applied as eye drops to each eye for 7 days. Naive mice did not receive the OVA challenge. Eyelid edema, tearing/discharge, chemosis and hyperemia were scored individually on a 0–3+ scale in a masked fashion 20 min after challenge each day for the 7 days of challenge.

DNA extraction and bacterial 16S rRNA gene sequencing

Detailed procedures DNA extraction, amplification, 16S rRNA gene sequencing, and data processing are provided in Supplementary materials and methods. Laboratory environmental samples along with blank extractions and reagents used at the time of amplification were also processed and analyzed as potential sources of contamination.

Microbiome data analysis

Based on the OTU information, α-diversity metrics of the Shannon index were calculated with QIIME software package. Bray–Curtis dissimilarities were produced as β-diversity measures and subjected to principal coordinate analysis (PCoA) with the vegan package and QIIME software package. Different groups were statistically compared using the similarity analysis, ANOSIM. The overlap of the microbial communities was determined by the R values from the ANOSIM according to the method of Buttigieg and Ramette[68]. To address the risk of contamination during the analysis of low-biomass samples, we employed the indicspecies R package to evaluate the specificity of an OTU with respect to the conjunctiva or the negative control[33,69]. This was achieved by calculating its IndVal index, which helped identify potential contaminants[17]. OTUs linked to negative controls were designated as contaminants and subsequently excluded from the analysis.

Microbial source tracking (FEAST)[70] was applied to predict the sources of the microbial communities detected in each of the six time points investigated across weeks 1-to-8. The co-occurrence networks were constructed to explore the internal community relationships across the samples[18]. In order to visualize associations in the network, we constructed a correlation matrix by calculating the possible pairwise Spearman's rank correlations. A correlation between two nodes was considered to be statistically robust if the Spearman's correlation coefficient was over 0.6 or less than −0.6 and the $P < 0.01$. The correlation networks were visualized using Gephi software. All microbiome analyses were conducted in R (version 4.2.3, R Development Core Team) unless otherwise stated.

Whole-mount immunostaining

Freshly harvested whole-mount conjunctival tissue obtained at each developmental stage were fixed with cold acetone at −20 °C and later stained as described in a previous study[71] using primary anti-CD45 (1:150), anti-CD11b (1:200), anti-CD11c (1:200), anti-MHC II (1:100) or anti-Keratin7 (Krt7, 1:100) antibodies. Digital confocal images were captured using a laser scanning confocal microscope (FV1000MPE-B, Olympus, Japan) and a 1.16 µm Z-step. The images were processed using FV10-ASW 4.2 viewer (Olympus). The antibodies used are shown in Table S5.

Flow cytometry and analysis

Conjunctival tissues were excised and exposed to 1 mg/ml collagenase (Roche, 11088866001) for 1 h at 37 °C to obtain cell suspensions, which were stained with anti-CD45 antibodies at 4 °C for 30 min. A CytoFLEX S Flow

Cytometer (Beckman Coulter, Indianapolis, IN, USA) was used and data were plotted and quantified with FlowJo software (FlowJo LLC, Ashland, OR, USA). The antibodies used are shown in Table S5. The gating strategy are shown in Fig. S7.

CLNs were collected from freshly euthanized mice and processed. Single cell suspensions were prepared and 10^6 cells were stimulated for 4 h with leukocyte activation cocktail (BD Pharmingen, 550583). Cells were stained with Fixable Viability Dye and surface antigen CD45, CD3, CD4, and CD25 for 30 min on ice. For intracellular staining, cells were prepared with transcription factor buffer (BD Pharmingen, 562574) and subsequently stained with IL-4 and IFN-γ antibodies. Data were acquired on SONY ID7000™ Spectral Cell Analyzer using the ID A analysis software (v2.0; SONY). Data were analyzed on FlowJo software (FlowJo LLC, Ashland, OR, USA). The antibodies used are shown in Table S5. The gating strategy are shown in Fig. S7.

In vivo administration of fluorescent antigens

A 2.5 µl eye drop of ovalbumin Alexafluor 647 (O34784, Thermofisher) was applied to each eye. The mice were then euthanized by cervical dislocation 30 min later. Whole-mount freshly harvested conjunctival tissues were fixed with cold methanol at −20 °C for 10 min and stained using Hoechst dye.

Histology

Eyes, including eyelid and conjunctival tissues from each group, were surgically excised and embedded in optimal cutting temperature (OCT) compound or paraffin, cut into sagittal sections (5 µm thick), and stored at −80 °C (frozen sections) or room temperature (paraffin sections). Hematoxylin and Eosin staining, PAS staining, Immunohistochemical staining, Picrosirius Red staining and Toluidine Blue staining were performed on paraffin sections. Immunofluorescence staining and TUNEL assay were performed on the frozen sections.

Examination of conjunctival goblet cells

For PAS staining, paraffin sections were stained using a PAS staining Kit (395B-1 KT, Sigma) according to the manufacturer's instructions. The superior and inferior conjunctiva were then examined and photographed with a digital light microscope (Eclipse 50i; Nikon, Tokyo, Japan) and the mucin-filled goblet cells counted. Three sections from each of the nasal, central and lateral parts of the eye from each animal were studied. For moxifloxacin-based fluorescence imaging, moxifloxacin ophthalmic solution (Vigamox, Alcon Laboratories, Fort Worth, USA) was used as a labeling agent, as previously reported[72]. The excised mouse conjunctival tissues were immersed in moxifloxacin ophthalmic solution for 3–5 min and imaged using a laser scanning confocal microscope (FV1000MPE-B, Olympus).

Immunofluorescent staining

For immunofluorescence staining, frozen sections were fixed in cold acetone at −20 °C for 10 min, followed by three washes with PBS for 5 min each and incubation in 0.2% Triton X-100 for 20 min. After washing the sections three times each with PBS for 5 min and pre-incubating with 2% bovine serum albumin (BSA) for 1 h at room temperature, sections were incubated with anti-Ki67 (1:300), anti-ZO-1 (1:200), anti-Krt19 (1:200), anti-MHC II (1:100) and anti-CD4 (1:200) antibodies for 16 h at 4 °C. The slides were then washed three times each with PBS for 10 min and incubated with secondary antibodies for 1 h in the dark at room temperature, followed by three washes each with PBS for 10 min. Sections were then counterstained with DAPI for 5 min, after which digital images of representative areas of the conjunctiva were taken with a laser scanning confocal microscope (FV1000MPE-B, Olympus). The antibodies used are shown in Table S5.

Quantitation of Sera IgE

Blood was collected from the submandibular vein of mice following topical challenge and serum was isolated. Total IgE was measured via ELISA, as per the manufacturer's instructions (EM024-96, ExCell, China).

Quantitative real-time PCR analysis

Total RNA from conjunctiva was extracted using the RNeasy Mini Kit (Qiagen) following the manufacturer's protocol. RNA quality was confirmed using Nanodrop (ThermoFisher) and reverse transcribed into cDNA by using a cDNA synthesis kit (RR047A; TakaRa, Japan). Quantitative PCR was performed with a Step One Plus Real-Time System (Applied Biosystems, Alameda, CA, USA). Table S6 provides the primer sequences used to amplify specific gene products. Expression data were normalized with β-actin as an endogenous reference.

Statistics and reproducibility

Statistical analyses were conducted with Prism 7 software (GraphPad, CA), without microbiome data analysis. The numbers of positive cells in whole-mount stained images of conjunctiva were measured using Image J (NIH). Unpaired two-tailed Student's *t* test was used to assess the difference between the two groups. For continuous variables of three groups or more, a one-way analysis of variance (ANOVA) test with a Tukey-adjusted pairwise comparison was performed. Data are expressed as means ± SEM. No statistical method was used to predetermine sample size of conjunctival 16S rRNA sequencing. We determined sample sizes by referring to previously published paper in the field[73]. *P* values of <0.05 were considered significant. Exact *P* values are provided in the source data (Supplementary Data).

Reporting summary

Further information on research design is available in the Nature Portfolio Reporting Summary linked to this article.

Data availability

All study data have been comprehensively incorporated within the article and/or Supplementary Information. The datasets of 16S rRNA genes generated during the current study have been deposited in the NCBI Sequence Read Archive (SRA) database (Accession Number: PRJNA923858). The source data behind the graphs in the main figures are provided in Supplementary Data. The other data are available from the corresponding author on reasonable request.

Received: 28 October 2024; Accepted: 18 October 2025;
Published online: 26 November 2025

References

1. Kugadas, A. & Gadjeva, M. Impact of microbiome on ocular health. *Ocul. Surf.* **14**, 342–349 (2016).
2. Watters, G. A., Turnbull, P. R., Swift, S., Petty, A. & Craig, J. P. Ocular surface microbiome in meibomian gland dysfunction. *Clin. Exp. Ophthalmol.* **45**, 105–111 (2017).
3. Venugopal, R. et al. Conjunctival microbial flora in ocular Stevens-Johnson syndrome sequelae patients at a tertiary eye care center. *Cornea* **35**, 1117–1121 (2016).
4. Petrillo, F. et al. Characterization and comparison of ocular surface microbiome in newborns. *Microorganisms* **10**, 1390 (2022).
5. Cavuoto, K. M., Galor, A. & Banerjee, S. Anatomic characterization of the ocular surface microbiome in children. *Microorganisms* **7**, 259 (2019).
6. Cavuoto, K. M., Mendez, R., Miller, D., Galor, A. & Banerjee, S. Effect of clinical parameters on the ocular surface microbiome in children and adults. *Clin. Ophthalmol.* **12**, 1189–1197 (2018).
7. Chen, F. V., Chang, T. C. & Cavuoto, K. M. Patient demographic and microbiology trends in bacterial conjunctivitis in children. *J. AAPOS* **22**, 66–67 (2018).
8. Pak, K. Y., Kim, S. I. & Lee, J. S. Neonatal bacterial conjunctivitis in Korea in the 21st century. *Cornea* **36**, 415–418 (2017).
9. Darling, E. K. & McDonald, H. A meta-analysis of the efficacy of ocular prophylactic agents used for the prevention of gonococcal and chlamydial ophthalmia neonatorum. *J. Midwifery Women's. Health* **55**, 319–327 (2010).

10. Bomar, L., Brugger, S. D. & Lemon, K. P. Bacterial microbiota of the nasal passages across the span of human life. *Curr. Opin. Microbiol.* **41**, 8–14 (2018).
11. Capone, K. A., Dowd, S. E., Stamatas, G. N. & Nikolovski, J. Diversity of the human skin microbiome early in life. *J. Investig. Dermatol.* **131**, 2026–2032 (2011).
12. Stewart, C. J. et al. Temporal development of the gut microbiome in early childhood from the TEDDY study. *Nature* **562**, 583–588 (2018).
13. Blaser, M. J. The theory of disappearing microbiota and the epidemics of chronic diseases. *Nat. Rev. Immunol.* **17**, 461–463 (2017).
14. Gensollen, T., Iyer, S. S., Kasper, D. L. & Blumberg, R. S. How colonization by microbiota in early life shapes the immune system. *Science* **352**, 539–544 (2016).
15. Russell, S. L. et al. Early life antibiotic-driven changes in microbiota enhance susceptibility to allergic asthma. *EMBO Rep.* **13**, 440–447 (2012).
16. Al Nabhani, Z. et al. A weaning reaction to microbiota is required for resistance to immunopathologies in the adult. *Immunity* **50**, 1276–1288.e1275 (2019).
17. Ozkan, J. et al. Biogeography of the human ocular microbiota. *Ocul. Surf.* **17**, 111–118 (2019).
18. Sun, H., Chen, F., Hao, H. & Wang, K. J. Multi-dimensional investigation and distribution characteristics analysis of gut microbiota of different marine fish in Fujian Province of China. *Front. Microbiol.* **13**, 918191 (2022).
19. Bian, F. et al. Age-associated antigen-presenting cell alterations promote dry-eye inducing Th1 cells. *Mucosal Immunol.* **12**, 897–908 (2019).
20. Gupta, D., Harvey, S. A., Kaminski, N. & Swamynathan, S. K. Mouse conjunctival forniceal gene expression during postnatal development and its regulation by Kruppel-like factor 4. *Investig. Ophthalmol. Vis. Sci.* **52**, 4951–4962 (2011).
21. Knoop, K. A. et al. Microbial antigen encounter during a preweaning interval is critical for tolerance to gut bacteria. *Sci. Immunol.* **2**, eaao1314 (2017).
22. Barbosa, F. L. et al. Goblet cells contribute to ocular surface immune tolerance-implications for dry eye disease. *Int. J. Mol. Sci.* **18**, 978 (2017).
23. Tukler Henriksson, J., Coursey, T. G., Corry, D. B., De Paiva, C. S. & Pflugfelder, S. C. IL-13 stimulates proliferation and expression of mucin and immunomodulatory genes in cultured conjunctival goblet cells. *Investig. Ophthalmol. Vis. Sci.* **56**, 4186–4197 (2015).
24. Al Nabhani, Z. & Eberl, G. Imprinting of the immune system by the microbiota early in life. *Mucosal Immunol.* **13**, 183–189 (2020).
25. Saban, D. R. et al. Resolvin D1 treatment on goblet cell mucin and immune responses in the chronic allergic eye disease (AED) model. *Mucosal Immunol.* **12**, 145–153 (2019).
26. Yau, J. W. et al. Characterization of ocular and nasopharyngeal microbiome in allergic rhinoconjunctivitis. *Pediatr. Allergy Immunol.* **30**, 624–631 (2019).
27. Cavuoto, K. M., Banerjee, S., Miller, D. & Galor, A. Composition and comparison of the ocular surface microbiome in infants and older children. *Transl. Vis. Sci. Technol.* **7**, 16 (2018).
28. Eder, M. et al. Normal ocular flora in newborns delivered in two hospital centers in Argentina and Paraguay. *Graefes Arch. Clin. Exp. Ophthalmol.* **243**, 1098–1107 (2005).
29. Isenberg, S. J., Apt, L., Yoshimori, R., Ward McCarty, J. & Alvarez, S. R. Source of the conjunctival bacterial flora at birth and implications for ophthalmia neonatorum prophylaxis. *Am. J. Ophthalmol.* **106**, 458–462 (1988).
30. Wen, X. et al. The influence of age and sex on ocular surface microbiota in healthy adults. *Investig. Ophthalmol. Vis. Sci.* **58**, 6030–6037 (2017).
31. Koenig, J. E. et al. Succession of microbial consortia in the developing infant gut microbiome. *Proc. Natl. Acad. Sci. USA* **108**, 4578–4585 (2011).
32. Yatsunenko, T. et al. Human gut microbiome viewed across age and geography. *Nature* **486**, 222–227 (2012).
33. Salter, S. J. et al. Reagent and laboratory contamination can critically impact sequence-based microbiome analyses. *BMC Biol.* **12**, 87 (2014).
34. Pei, Y. F. & Rhodin, J. A. The prenatal development of the mouse eye. *Anat. Rec.* **168**, 105–125 (1970).
35. Harris-Tryon, T. A. & Grice, E. A. Microbiota and maintenance of skin barrier function. *Science* **376**, 940–945 (2022).
36. St Leger, A. J. et al. An ocular commensal protects against corneal infection by driving an interleukin-17 response from mucosal γδ T cells. *Immunity* **47**, 148–158.e145 (2017).
37. Torow, N. & Hornef, M. W. The neonatal window of opportunity: setting the stage for life-long host-microbial interaction and immune homeostasis. *J. Immunol.* **198**, 557–563 (2017).
38. Chisari, G., Chisari, E. M., Borzi, A. M. & Chisari, C. G. Aging eye microbiota in dry eye syndrome in patients treated with *Enterococcus faecium* and *Saccharomyces boulardii*. *Curr. Clin. Pharm.* **12**, 99–105 (2017).
39. Ignacio, A., Czyz, S. & McCoy, K. D. Early life microbiome influences on development of the mucosal innate immune system. *Semin. Immunol.* **73**, 101885 (2024).
40. Ohnmacht, C. et al. MUCOSAL IMMUNOLOGY. The microbiota regulates type 2 immunity through RORγt^{+} T cells. *Science* **349**, 989–993 (2015).
41. Yang, B. H. et al. Foxp3(+) T cells expressing RORγt represent a stable regulatory T-cell effector lineage with enhanced suppressive capacity during intestinal inflammation. *Mucosal Immunol.* **9**, 444–457 (2016).
42. Contreras-Ruiz, L. & Masli, S. Immunomodulatory cross-talk between conjunctival goblet cells and dendritic cells. *PLoS ONE* **10**, e0120284 (2015).
43. Alam, J., de Paiva, C. S. & Pflugfelder, S. C. Immune-goblet cell interaction in the conjunctiva. *Ocul. Surf.* **18**, 326–334 (2020).
44. Logeswaran, A., Contreras-Ruiz, L. & Masli, S. Conjunctival goblet cell responses to TLR5 engagement promote activation of local antigen-presenting cells. *Front. Immunol.* **12**, 716939 (2021).
45. Niess, J. H. et al. CX3CR1-mediated dendritic cell access to the intestinal lumen and bacterial clearance. *Science* **307**, 254–258 (2005).
46. Iwasaki, A. Mucosal dendritic cells. *Annu Rev. Immunol.* **25**, 381–418 (2007).
47. Perner, C. et al. Substance P release by sensory neurons triggers dendritic cell migration and initiates the type-2 immune response to allergens. *Immunity* **53**, 1063–1077.e1067 (2020).
48. Knoop, K. A., McDonald, K. G., McCrate, S., McDole, J. R. & Newberry, R. D. Microbial sensing by goblet cells controls immune surveillance of luminal antigens in the colon. *Mucosal Immunol.* **8**, 198–210 (2015).
49. Kimura, M. et al. A nerve-goblet cell association promotes allergic conjunctivitis through rapid antigen passage. *JCI Insight* **8**, e168596 (2023).
50. Tamburini, S., Shen, N., Wu, H. C. & Clemente, J. C. The microbiome in early life: implications for health outcomes. *Nat. Med.* **22**, 713–722 (2016).
51. Bashir, M. E., Louie, S., Shi, H. N. & Nagler-Anderson, C. Toll-like receptor 4 signaling by intestinal microbes influences susceptibility to food allergy. *J. Immunol.* **172**, 6978–6987 (2004).
52. Gollwitzer, E. S. et al. Lung microbiota promotes tolerance to allergens in neonates via PD-L1. *Nat. Med.* **20**, 642–647 (2014).
53. Lee, Y. S. et al. Microbiota-derived lactate accelerates intestinal stem-cell-mediated epithelial development. *Cell Host Microbe* **24**, 833–846.e836 (2018).

54. Wang, C. et al. Sjögren-like lacrimal keratoconjunctivitis in germ-free mice. *Int. J. Mol. Sci.* **19**, 565 (2018).
55. Lynn, M. A. et al. Early-life antibiotic-driven dysbiosis leads to dysregulated vaccine immune responses in mice. *Cell Host Microbe* **23**, 653–660 e655 (2018).
56. Xue, R. et al. Temporal impacts of topical ceftazidime and tobramycin-vancomycin mixtures on the ocular surface microbiota in rabbits. *Exp. Eye Res.* **220**, 109098 (2022).
57. Langdon, A., Crook, N. & Dantas, G. The effects of antibiotics on the microbiome throughout development and alternative approaches for therapeutic modulation. *Genome Med.* **8**, 39 (2016).
58. Littmann, E. R. et al. Host immunity modulates the efficacy of microbiota transplantation for treatment of Clostridioides difficile infection. *Nat. Commun.* **12**, 755 (2021).
59. Azad, M. B. et al. Infant gut microbiota and food sensitization: associations in the first year of life. *Clin. Exp. Allergy* **45**, 632–643 (2015).
60. Russell, S. L. et al. Perinatal antibiotic treatment affects murine microbiota, immune responses and allergic asthma. *Gut Microbes* **4**, 158–164 (2013).
61. Donald, K. & Finlay, B. B. Early-life interactions between the microbiota and immune system: impact on immune system development and atopic disease. *Nat. Rev. Immunol.* **23**, 735–748 (2023).
62. Kuo, C. H. et al. Early life exposure to antibiotics and the risk of childhood allergic diseases: an update from the perspective of the hygiene hypothesis. *J. Microbiol. Immunol. Infect.* **46**, 320–329 (2013).
63. Oyama, N., Sudo, N., Sogawa, H. & Kubo, C. Antibiotic use during infancy promotes a shift in the T(H)1/T(H)2 balance toward T(H)2-dominant immunity in mice. *J. Allergy Clin. Immunol.* **107**, 153–159 (2001).
64. Das, A. V., Donthineni, P. R., Sai Prashanthi, G. & Basu, S. Allergic eye disease in children and adolescents seeking eye care in India: electronic medical records driven big data analytics report II. *Ocul. Surf.* **17**, 683–689 (2019).
65. Pawankar, R. Allergic diseases and asthma: a global public health concern and a call to action. *World Allergy Organ J.* **7**, 12 (2014).
66. Cavuoto, K. M., Stradiotto, A. C. & Galor, A. Role of the ocular surface microbiome in allergic disease. *Curr. Opin. Allergy Clin. Immunol.* **19**, 482–487 (2019).
67. Minich, J. J. et al. KatharoSeq enables high-throughput microbiome analysis from low-biomass samples. *mSystems* **3**, e00218 (2018).
68. Buttigieg, P. L. & Ramette, A. A guide to statistical analysis in microbial ecology: a community-focused, living review of multivariate data analyses. *FEMS Microbiol. Ecol.* **90**, 543–550 (2014).
69. De Cáceres, M. & Legendre, P. Associations between species and groups of sites: indices and statistical inference. *Ecology* **90**, 3566–3574 (2009).
70. Shenhav, L. et al. FEAST: fast expectation-maximization for microbial source tracking. *Nat. Methods* **16**, 627–632 (2019).
71. Ko, B. Y. Xiao, Y. Barbosa, F. L. de Paiva, C. S. & Pflugfelder, S. C. Goblet cell loss abrogates ocular surface immune tolerance. *JCI Insight* **3**, e98222 (2018).
72. Kim, S. et al. In vivo fluorescence imaging of conjunctival goblet cells. *Sci. Rep.* **9**, 15457 (2019).
73. Singh, N., Vats, A., Sharma, A., Arora, A. & Kumar, A. The development of lower respiratory tract microbiome in mice. *Microbiome* **5**, 61 (2017).

Acknowledgements

The authors thank Jingru Huang, Haiping Zheng, Baoying Xie and Xiang You from the Core Facility of Biomedical Science, Xiamen University for technical support. This study is supported, in part, by the National Key R&D Program of China (2018YFA0107301 to W.L.), the National Natural Science Foundation of China (NSFC; No. 81770894 to W.L., No. 81970773 to W.L. and No. 82471047 to W.L.), the Fujian Provincial Natural Science Foundation of China (No. 2025J011398 to Y.L.) and the Xiamen Health and Wellness High-Quality Development Science and Technology Program (No. 2024GZL-QN004 to Y.L.). The funders played no role in the study design, data collection and analysis, decision on publishing or preparation of the manuscript.

Author contributions

Y.L., H.S., S.S., and W.L. designed research; Y.L., H.S., S.S., X.H. and H.W. (Han Wu) performed research and the data analysis; G.F., Y.W., Z.L., H.W. (Huping Wu) and W.L. supervised the work and analyzed the data; S.O., R.Z., H.H., and Y.C. contributed reagents, materials, and analytic tools; Y.L., A.J.Q., and W.L. wrote the paper with the contribution of all authors. All authors read and approved the final manuscript.

Competing interests

The authors declare no competing interests.

Additional information

Supplementary information The online version contains supplementary material available at https://doi.org/10.1038/s42003-025-09095-4.

Correspondence and requests for materials should be addressed to Wei Li.

Peer review information *Communications Biology* thanks the anonymous reviewers for their contribution to the peer review of this work. Primary handling editor: Dario Ummarino.